

Zero-Shot In-Distribution Detection in Multi-Object Settings Using Vision-Language Foundation Models

Atsuyuki Miyai¹ Qing Yu¹ Go Irie² Kiyoharu Aizawa¹

¹The University of Tokyo ²Tokyo University of Science

{miyai,yu,aizawa}@hal.t.u-tokyo.ac.jp goirie@ieee.org

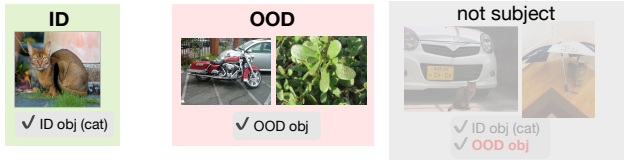
Abstract

Removing out-of-distribution (OOD) images from noisy images scraped from the Internet is an important preprocessing for constructing datasets, which can be addressed by zero-shot OOD detection with vision language foundation models (CLIP). The existing zero-shot OOD detection setting does not consider the realistic case where an image has both in-distribution (ID) objects and OOD objects. However, it is important to identify such images as ID images when collecting the images of rare classes or ethically inappropriate classes that must not be missed. In this paper, we propose a novel problem setting called in-distribution (ID) detection, where we identify images containing ID objects as ID images, even if they contain OOD objects, and images lacking ID objects as OOD images. To solve this problem, we present a new approach, **Global-Local Maximum Concept Matching (GL-MCM)**, based on both global and local visual-text alignments of CLIP features, which can identify any image containing ID objects as ID images. Extensive experiments demonstrate that GL-MCM outperforms comparison methods on both multi-object datasets and single-object ImageNet benchmarks.

1. Introduction

The basic process for constructing datasets is to collect images from the Internet and manually annotate them [2]. Because many non-target (out-of-distribution) images are included among images scrapped from the Internet, considerable human effort is required to check all the collected images and exclude out-of-distribution (OOD) images. To apply deep learning techniques for the preprocessing to remove OOD from the collected images, a system that can distinguish between in-distribution (ID) and OOD without training on ID images is required. Recently, the development of vision language foundation models (e.g., CLIP [28]) has enabled the detection of OOD images with only ID class names, which is a research area known as

Existing setting (Zero-shot OOD detection)



Our setting (Zero-shot ID detection)

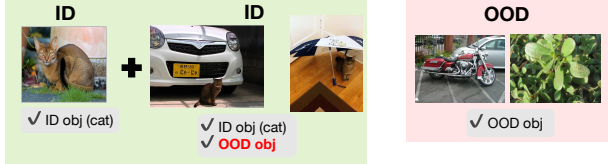


Figure 1: **Our experimental settings** of in-distribution (ID) detection. Unlike the existing setting, our setting deals with the case where OOD objects are found in the image. In this setting, we want the model to identify such images as ID images.

zero-shot OOD detection [8, 6, 23]. Although zero-shot OOD detection has been studied for the purpose of detecting OOD when deploying machine learning models in the field, it can also be used in the preprocessing of dataset construction. Using this zero-shot OOD detector for dataset construction is valuable because it can significantly reduce the human effort required to remove unnecessary OOD images from a dataset before annotating them.

The existing setting for zero-shot OOD detection has some limitations for use in dataset construction. That is, an ID image contains only ID objects, as shown in Fig. 1 (upper). In reality, this is not the case, and many images contain both ID and OOD objects, as shown in Fig. 1 (bottom). When using a zero-shot OOD detector for the cleaning of collected data, images containing ID and OOD objects need to be identified as ID images when collecting images in rare classes or ethically inappropriate classes for which instances should not be missed. If images containing such class objects are excluded as OOD images at the data

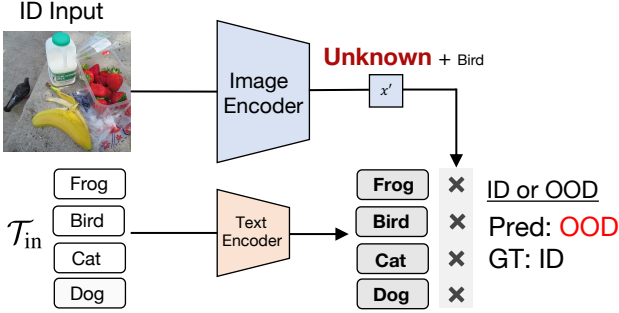


Figure 2: **Limitation of existing work** (*i.e.*, MCM [23]). When OOD objects appear in the ID image, the image feature might be occupied by information of OOD objects instead of the ID object (in this case, a bird).

cleaning stage, a large amount of human cost is required to find such images among many excluded OOD images. Therefore, a system that can correctly identify images containing ID objects as ID images, even if they contain OOD objects, is crucial for real-world applications.

In this paper, we propose a novel setting where we identify images containing ID objects as ID images even if they contain OOD objects and images without ID objects as OOD images. We name our problem setting “in-distribution (ID) detection”. Note that ID detection and OOD detection have the same goal of distinguishing ID and OOD images, so the zero-shot OOD detection method can serve as a baseline.

In our ID detection setting, we find that existing zero-shot OOD detection methods [8, 6, 23] do not perform well. For example, the state-of-the-art method MCM [23] identifies ID and OOD images by calculating the confidence scores with the softmax score, which is based on the similarities between the global image feature and ID class textual features. However, in our ID detection setting, MCM might not distinguish ID images from OOD images because the CLIP’s image encoder generates features for both ID and OOD objects, leading to a blending of ID and OOD concepts within the global image features, as shown in Fig. 2. In particular, when the OOD object is dominant in the ID image, MCM incorrectly judges the image as an OOD image.

We propose a simple yet effective approach to solve this problem. As an analysis of the CLIP encoder, we find that the use of spatial aggregation for embeddings of CLIP’s image encoder results in less ID information. Hence, we propose a solution that leverages the local feature without pooling to calculate the ID confidences since the local feature would have the information on all objects in the image. By projecting the value features of the last attention layer into the textual space, we can align local visual fea-

tures with textual concepts [40]. However, the local features alone cannot accurately evaluate the similarity of an image that contains larger ID objects because they are less likely to capture the global information of the image. Therefore, we propose Global-Local Maximum Concept Matching (GL-MCM), which incorporates both global and local visual-text alignments. GL-MCM utilizes both the global and local concept matching scores to compensate for the shortcomings of both visual-text alignments, which can identify any image containing ID objects as ID images regardless of whether ID objects appear globally or locally.

We evaluated our methods on multi-object data created from the MS-COCO [20] and Pascal-VOC [7] datasets. In our novel setting, our proposed GL-MCM outperforms MCM. Furthermore, even on the single-object ImageNet OOD benchmarks [15], our proposed GL-MCM is comparable or superior to other detection methods.

The contributions of our paper are summarized as follows:

- We propose a novel problem called in-distribution detection, where we identify images containing ID objects as ID images, even if they contain OOD objects, and images lacking ID objects as OOD images. (see Fig. 1).
- We propose GL-MCM, a simple yet effective method based on global and local vision-language concept alignments (see Fig. 3).
- In both multi-object settings and single-object settings, our GL-MCM outperforms the existing detection methods (see Table 1, Table 2, and Fig. 4).
- We provide ID detection datasets from MS-COCO and Pascal-VOC to encourage further research.

2. Related Work

2.1. Out-of-distribution detection

Single-modal supervised OOD detection. Various approaches have been developed to address OOD detection in computer vision [9, 16, 24, 25, 26, 12, 11, 14, 19, 32, 21, 17, 34, 38] and natural language processing [13, 27, 37]. However, these OOD detection methods assume the use of backbones trained with single-modal data, so they require task-specific training costs.

Multi-modal zero-shot OOD detection. To overcome the limitations of single-modal supervised OOD detection, CLIP-based zero-shot OOD detection has been proposed [8, 6, 23]. There are two approaches for zero-shot OOD detection: using OOD labels (known labels [8] or pseudo-labels [6]) or not using OOD labels [23] to calculate the ID confidence score. As for the approaches to using

OOD labels, the earliest work is Fort *et al.* [8]. Fort *et al.* assumed that the classes of OOD images \mathcal{Y}_{ood} are known and used $\sum_{y \in \mathcal{Y}_{\text{ood}}} \hat{p}(y | \mathbf{x})$ for detecting OOD images, where $\hat{p}(y | \mathbf{x})$ is calculated by normalizing the inner products over $\mathcal{Y}_{\text{id}} + \mathcal{Y}_{\text{ood}}$ classes. However, knowing OOD labels is generally not feasible, so it is not realistic to apply this approach to the real world. The next work is ZOC [6], which developed Fort’s method [8] by using generated pseudo-OOD candidate labels with a text generation model. However, as described by MCM [23], the generated OOD labels have some overlap with ID labels. In addition, all generated labels are used as OOD labels, so it is not possible to detect ID images containing OOD objects. To overcome the problems with methods using OOD labels, MCM, a method that does not use OOD labels, has been proposed. MCM identifies ID and OOD images by calculating the confidence scores with the softmax score. Despite its simplicity, MCM greatly outperforms the performance of ZOC, which indicates that the methods not using OOD labels are beneficial. MCM is possible to apply to our setting, but its detection performance becomes suboptimal because MCM uses only global features to identify ID images.

2.2. Multi-object out-of-distribution detection

The existing settings for multi-object OOD detection are multi-label OOD detection [11, 35] and multi-object OOD object detection [5, 4]. In this section, we describe the differences between these settings and our setting.

Multi-label OOD detection. The motivation of multi-label OOD detection [11, 35] is to detect OOD images when the given ID image has multiple ID objects and does not have any OOD objects. They explored OOD detection methods with a multi-label classifier instead of a single-label classifier. The major difference between the multi-label OOD setting and our setting is that, in the multi-label OOD setting, there are no OOD objects in the given ID image, whereas, in our ID detection setting, some OOD objects appear in the ID image.

Multi-object OOD object detection. The motivation of multi-object OOD object detection [5, 4] is to describe the spatial location of ID and OOD objects with a bounding box. This task requires training an object detector with detailed annotation data. However, in the real world, it costs a lot of human effort to create detailed annotation data, especially for large-scale datasets. Besides, when cleaning datasets, there is no need to describe the location of an object in detail, and we only need to know if ID objects are included. Therefore, it is important to develop a method to determine whether ID objects are included in the given image by zero-shot prediction.

2.3. Vision-language models

Utilizing large-scale pre-trained vision-language models such as CLIP [28] and ALIGN [18] for multimodal downstream tasks has become an emerging paradigm with remarkable performance. CLIP [28] pre-trains an image and language encoder pair on large-scale data containing hundreds of millions of image-caption pairs. Since these models have rich visual and text alignment features, they can be applied to diverse tasks, such as zero-shot classification [28, 22], few-shot classification [42, 41], OOD detection [23] and various other tasks [30, 31, 40]. In this work, we present a novel approach to adapt CLIP to ID detection without any additional training.

3. Methodology

In this section, we present our proposed method. First, we define the problem in Section 3.1. Second, we explain the overview and limitation of MCM in Section 3.2. Finally, we explain our proposed method GL-MCM in Section 3.3.

3.1. Problem statements

Zero-shot ID detection and zero-shot OOD detection have the same goal of separating ID and OOD images without ID training. For zero-shot ID detection and OOD detection, the ID classes refer to the classes used in the downstream classification task, which are different from the classes of the upstream pre-training. Accordingly, OOD classes are the classes that do not belong to any of the ID classes of the downstream task. Both the ID detector and OOD detector can be viewed as a binary classifier that identifies whether the image is an ID image or an OOD image. Different from the zero-shot OOD setting, the OOD detection setting considers only the case that the ID image has only ID objects, whereas, in our zero-shot ID detection setting, we consider images containing both ID and OOD objects as ID images. This study aims to identify images containing both ID and OOD objects as ID images and images not containing ID objects as OOD images.

3.2. Preliminaries of MCM

Overview of MCM. MCM [23] calculates the confidence scores with the softmax score of the similarity between global image features and class textual features. For CLIP’s image encoder (*i.e.*, modified ResNet), the original attention pooling layer pools the visual feature map first and then projects the global feature vector into text space by $\text{Proj}_{v \rightarrow t}$. We define the visual and textual encoders as $E_v(\cdot)$ and $E_t(\cdot)$. For any test input image, we define the output feature map of $E_v(\cdot)$ as $\mathbf{x} \in \mathbb{R}^{H \times W \times C}$, where H, W, and C are the height, width and the number of channels of the feature maps. The detailed operation for creating the

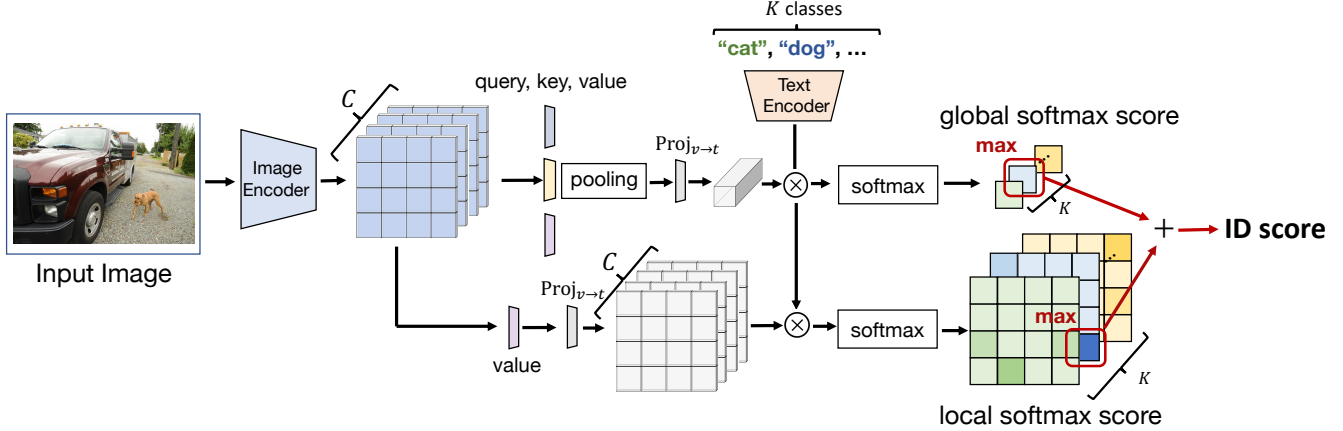


Figure 3: **Overview of the Global-Local Maximum Concept Matching (GL-MCM) framework.** Our approach utilizes both global and local softmax scores to calculate the ID confidence. By incorporating both global and local scores, our framework compensates for the respective weaknesses of the global and local alignments.

global feature $\mathbf{x}' \in \mathbb{R}^C$ is as follows:

$$\begin{aligned} \mathbf{x}' &= \text{AttnPool}(\mathbf{x}) \\ &= \text{Proj}_{v \rightarrow t} \left(\sum_i \text{softmax} \left(\frac{q(\bar{\mathbf{x}})k(\mathbf{x}_i)^T}{D} \right) \cdot v(\mathbf{x}_i) \right), \end{aligned} \quad (1)$$

where q , v , and k denote the query, value, and key, and they are independent linear embedding layers in CLIP. D is a constant scaling factor. $\bar{\mathbf{x}} \in \mathbb{R}^C$ is created by applying global average pooling to \mathbf{x} . $\mathbf{x}_i \in \mathbb{R}^C$ denotes the visual feature of each region i of feature map \mathbf{x} .

Let \mathcal{T}_{in} denote the set of test prompts containing K class labels (e.g., “a photo of a [CLASS]”). The output text feature for $t \in \mathcal{T}_{\text{in}}$ is defined as $\mathbf{y}_t = E_t(t)$. The score function of MCM is defined as follows:

$$S_{\text{MCM}} = \max_{t \in \mathcal{T}_{\text{in}}} \frac{e^{\text{sim}(\mathbf{x}', \mathbf{y}_t)/\tau}}{\sum_{c \in \mathcal{T}_{\text{in}}} e^{\text{sim}(\mathbf{x}', \mathbf{y}_c)/\tau}}, \quad (2)$$

where $\text{sim}(\mathbf{u}_1, \mathbf{u}_2) = \mathbf{u}_1 \cdot \mathbf{u}_2 / \|\mathbf{u}_1\| \cdot \|\mathbf{u}_2\|$ denote cosine similarity between \mathbf{u}_1 and \mathbf{u}_2 and τ is the temperature. Ming *et al.* [23] stated that softmax scaling improves the separability between ID and OOD images.

Limitations of MCM In Eq. 1, $\sum_i \text{softmax} \left(\frac{q(\bar{\mathbf{x}})k(\mathbf{x}_i)^T}{D} \right)$ is the attention map, which aggregates the feature map into the global feature. The major problem here is that the attention map in the pooling operation has no knowledge of which objects in the image are ID objects or OOD objects and has overall knowledge of the whole image. If the ID image is dominant compared to the OOD object, there is no problem. However, when the OOD object is dominant in the image, its global feature has less ID information, and MCM incorrectly judges the image as an OOD image.

3.3. Proposed approach

In the proposed approach, we leverage the local embeddings of CLIP for ID detection. In the original attention pooling layer in CLIP, we can replace the projection into text space $\text{Proj}_{v \rightarrow t}$ and the pooling operation as follows:

$$\begin{aligned} \text{AttnPool}(\mathbf{x}) &= \text{Proj}_{v \rightarrow t} \left(\sum_i \text{softmax} \left(\frac{q(\bar{\mathbf{x}})k(\mathbf{x}_i)^T}{D} \right) \cdot v(\mathbf{x}_i) \right) \\ &= \sum_i \text{softmax} \left(\frac{q(\bar{\mathbf{x}})k(\mathbf{x}_i)^T}{D} \right) \cdot \text{Proj}_{v \rightarrow t}(v(\mathbf{x}_i)) \\ &= \text{Pool}(\text{Proj}_{v \rightarrow t}(v(\mathbf{x}_i))), \end{aligned} \quad (3)$$

where q , v and k are independent linear embedding layers and $\text{Pool}(\cdot)$ denotes $\sum_i \text{softmax} \left(\frac{q(\bar{\mathbf{x}})k(\mathbf{x}_i)^T}{D} \right)$.

By removing the pooling operation in Eq. 3, we can project the visual feature \mathbf{x}_i of each region i to the textual space [40]:

$$\mathbf{x}'_i = \text{Proj}_{v \rightarrow t}(v(\mathbf{x}_i)). \quad (4)$$

For ViT, we can also obtain this feature map with similar procedures [40]. This feature has a rich local visual and textual alignment [40]. However, this local feature map calculates the similarity pixel-by-pixel, so it might be difficult to calculate the accurate similarity to the global object appearing over many pixels. Therefore, we propose a simple yet effective ID detection method called Global-Local Maximum Concept Matching (GL-MCM), which incorporates both global and local features. In Fig. 3, we show the overview of GL-MCM. For local alignments, we extend the concepts of MCM for local alignment features, and we first propose Local Maximum Concept Matching (L-MCM), in which we characterize ID confidences by the closest distance between the local visual text concept similarities. The

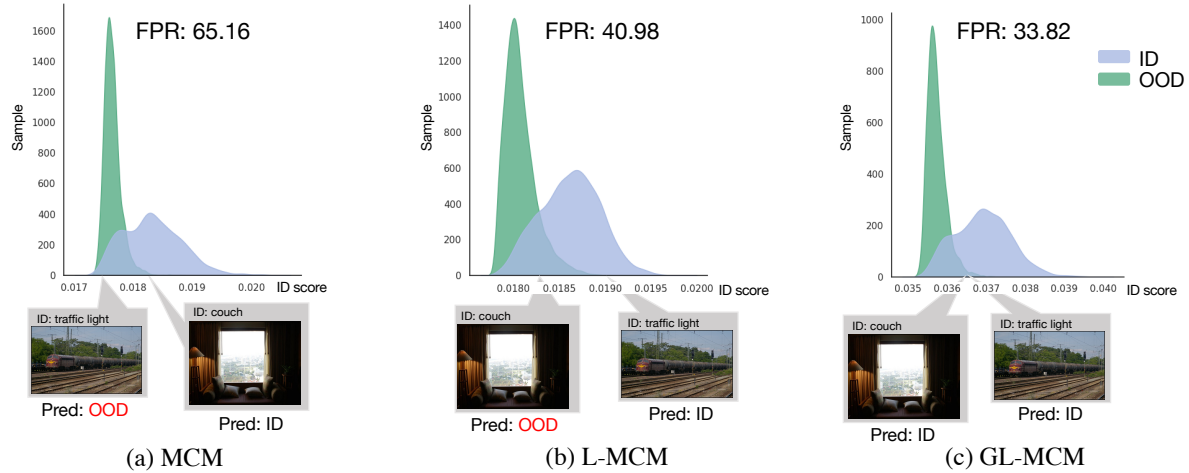


Figure 4: **Comparison of the histograms of ID confidences.** We use MS-COCO (ID) and iNaturalist (OOD). We use CLIP-ViT-B/16. We observe that GL-MCM has the least overlapping areas of ID and OOD than MCM and L-MCM. In addition, we found that GL-MCM can identify the ID images, which either MCM or L-MCM can mistake.

score function for local matching is defined as follows:

$$S_{L-MCM} = \max_{t,i} \frac{e^{\text{sim}(\mathbf{x}'_i, \mathbf{y}_t)/\tau}}{\sum_{c \in \mathcal{T}_{in}} e^{\text{sim}(\mathbf{x}'_i, \mathbf{y}_c)/\tau}}. \quad (5)$$

Then, we propose GL-MCM, which ensembles the score functions of MCM for global objects and L-MCM for local objects. The score function for GL-MCM is defined as follows:

$$S_{GL-MCM} = S_{MCM} + S_{L-MCM}. \quad (6)$$

GL-MCM is a simple ensembled method, yet it can accurately compensate for the respective weaknesses of the global and local score functions and improve the ability to identify ID images whenever ID objects appear globally or locally.

4. Experiment

4.1. Experimental Detail

ID Datasets. We mainly evaluate our proposals on two real-world datasets created from MS-COCO [20] and Pascal-VOC [7]. We split annotated classes into ID and OOD classes and created the dataset by collecting images that contain single-class ID objects and one or more class OOD objects in one image, as shown in Fig. 5. For our datasets, MS-COCO contains 5,000 images with 59 ID classes and 20 OOD classes, and Pascal-VOC contains 1,000 with 14 ID classes and 6 OOD classes. The detailed information on these datasets is shown in the supplementary. In the main experiments, each ID image contains single-class ID objects and does not contain multi-class ID

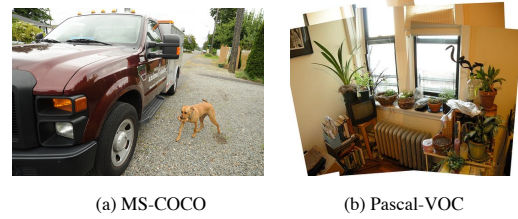


Figure 5: Examples of ID images created from the MS-COCO and Pascal-VOC datasets. For the above image in COCO, the ID object is a dog, and other objects (e.g., car) are OOD objects. For the above image in VOC, the ID object is a TV monitor, and other objects (e.g., potted plant) are OOD objects.

objects. There are two reasons. The first is that the motivation for collecting a dataset of single-label images (where single-class ID objects appear in each image) and that of collecting multi-label images (where multi-class ID objects appear in each image) is different, and it would be better to experiment on them separately. The second is that it is easier to identify ID images containing multi-class ID objects (which means more ID objects exist in the image) because the global image feature has more ID objects' information. Note that our method also gives much improvement even when multi-class ID objects appear in each image. The results are shown in the supplementary.

OOD Datasets. For OOD test datasets, we use iNaturalist [33], SUN [36], TEXTURE [1] and ImageNet-22K [29]. These datasets are used as OOD in the existing works [23, 15, 35]. However, these OOD data contain only

Table 1: **Main results.** We compare zero-shot ID detection performances on MS-COCO and Pascal-VOC. All values are percentages. Bold values represent the highest performance. We find that GL-MCM outperforms other methods in most settings.

(a) MS-COCO												
Method	iNaturalist		SUN		Texture		IN-22K		VOC		Average	
	FPR95↓	AUROC↑	FPR95↓	AUROC↑	FPR95↓	AUROC↑	FPR95↓	AUROC↑	FPR95↓	AUROC↑	FPR95↓	AUROC↑
ResNet-50												
MCM [23]	70.56	88.38	63.9	86.63	73.74	84.57	89.8	77.42	77.55	84.54	75.11	84.31
L-MCM (ours)	55.18	90.65	59.1	86.48	45.08	87.54	75.4	81.22	70.3	83.89	61.01	85.96
GL-MCM (ours)	55.74	92.17	54.7	88.96	49.76	88.78	80.5	82.23	71.15	86.77	62.37	87.78
ViT-B												
MCM [23]	65.16	91.03	84.94	82.27	67.36	86.63	80.02	84.8	79.2	84.47	75.34	85.84
L-MCM (ours)	40.98	92.42	50.72	89.38	84.96	74.83	75.04	78.50	71.03	84.18	64.55	83.86
GL-MCM (ours)	33.82	94.52	61.58	88.74	71.94	84.48	70.24	85.09	71.00	87.66	61.72	88.10
(b) Pascal-VOC												
Method	iNaturalist		SUN		Texture		IN-22K		COCO		Average	
	FPR95↓	AUROC↑	FPR95↓	AUROC↑	FPR95↓	AUROC↑	FPR95↓	AUROC↑	FPR95↓	AUROC↑	FPR95↓	AUROC↑
ResNet-50												
MCM [23]	15.5	96.88	30.3	93.77	54.5	89.66	58.0	90.34	56.1	89.11	42.88	91.95
L-MCM (ours)	19.4	97.24	29.7	94.55	27.0	95.77	50.5	93.05	55.6	89.2	36.44	93.96
GL-MCM (ours)	3.2	98.55	17.5	96.11	23.3	95.90	40.1	94.45	45.0	91.82	25.82	95.37
ViT-B												
MCM [23]	8.2	98.23	28.6	94.68	51.7	91.45	51.4	90.94	54.5	89.02	38.88	92.86
L-MCM (ours)	27.7	94.97	44.2	88.87	60.6	86.23	54.1	86.27	57.0	84.06	48.72	88.08
GL-MCM (ours)	4.2	98.71	23.1	94.66	43.0	92.84	41.0	92.38	44.3	90.48	31.12	93.81

a single class category, which might result in an oversimplified setup. Therefore, we also use multi-label OOD datasets subset of images from Pascal-VOC and MS-COCO. We use Pascal-VOC as OOD when the ID is MS-COCO and use MS-COCO as OOD when the ID is Pascal-VOC. Note that classes in ID do not overlap with the classes in OOD. For each OOD dataset, the classes are not overlapping with the ID classes. The detailed information on these datasets is shown in the supplementary.

Model. For the fields of OOD detection, both CNN-based models and Transformer-based models have been widely explored [8, 11]. Following this practice, we use ResNet-50 [10] and ViT-B/16 [3] as a backbone. Specifically, we use the publicly available CLIP-ResNet-50 and CLIP-ViT-B/16 models (<https://github.com/openai/CLIP>). The resolution of CLIP’s feature map is 7×7 for CLIP-ResNet-50 and 14×14 for CLIP-ViT-B/16. The temperature τ is 1 for all experiments following [23]. For the text prompts, we use “a photo of a [CLASS]”.

Comparison Methods. To evaluate the effectiveness of GL-MCM, we compare it with MCM. As another comparison method, we use the detection method using the local score function in Eq. 5, which is named L-MCM. As described in Section 2.1, other CLIP-based zero-shot OOD detection methods which use pseudo-OOD labels [8, 6] cannot

be directly applied to our ID detection setting. In addition, we do not consider creating new comparison methods by incorporating pseudo-OOD labels into our GL-MCM, because MCM [23] pointed out the poor quality of generated OOD labels and low detection performance. Instead, we conduct thorough experiments of the ablation studies for the score functions, which are most important for methods that do not use OOD labels, in Analysis Section 4.4.

Evaluation Metrics. For evaluation, we use the following metrics: (1) the false positive rate of OOD images when the true positive rate of in-distribution images is at 95% (FPR95), (2) the area under the receiver operating characteristic curve (AUROC).

4.2. Main Results

The zero-shot ID detection performance on MS-COCO and Pascal-VOC is summarized in Table 1. This result indicates that the method with the highest performance is GL-MCM. In addition to performance improvement, we can confirm that GL-MCM is a good ensemble method to reinforce each other’s weaknesses of MCM and L-MCM. As for the average AUROC scores, the superiority of AUROC scores by MCM and L-MCM depends on the datasets, but GL-MCM outperforms them in all settings.

In Fig. 4, we show the histograms of ID confidence

Table 2: **Comparison results on common ImageNet benchmarks.** The supervised methods are trained on ImageNet-1K. Zero-shot methods do not require any training with ImageNet-1K. We use CLIP-B/16 (ViT-B/16 for Fort [8]) as the backbone. Bold values represent the highest performance, and underlined values represent the second highest performance in each line. We find that GL-MCM is comparable or superior to other detection methods on single-object datasets.

Method	iNaturalist		SUN		Places		Texture		Average	
	FPR95↓	AUROC↑	FPR95↓	AUROC↑	FPR95↓	AUROC↑	FPR95↓	AUROC↑	FPR95↓	AUROC↑
Requires training (or w. fine-tuning)										
Fort <i>et al.</i> [8] (ViT-B)	15.07	96.64	54.12	86.37	57.99	85.24	53.32	84.77	45.12	88.25
MSP (CLIP-B) [12]	40.89	88.63	65.81	81.24	67.90	80.14	64.96	78.16	59.89	82.04
Energy (CLIP-B) [21]	21.59	95.99	<u>34.28</u>	93.15	36.64	91.82	51.18	88.09	<u>35.92</u>	92.26
Zero-shot (no training required)										
MCM [23]	30.91	94.61	37.59	92.57	44.69	89.77	57.77	86.11	42.74	90.77
L-MCM (ours)	49.19	86.96	73.65	76.62	79.14	71.86	92.39	59.48	73.59	73.73
GL-MCM (ours)	<u>15.18</u>	96.71	30.42	<u>93.09</u>	<u>38.85</u>	<u>89.90</u>	57.93	83.63	35.47	<u>90.83</u>

scores. This figure shows that GL-MCM has the least overlapping areas of ID and OOD than MCM and L-MCM. In addition, for the image where the ID object appears locally, MCM incorrectly judges the ID image as an OOD image. On the other hand, if the ID object appears globally, L-MCM incorrectly judges the ID image as an OOD image. However, since GL-MCM compensates for the shortcomings of both MCM and L-MCM, GL-MCM can correctly identify both images as ID images.

4.3. Results in single-object ID detection settings

In this section, we compare our proposal in the single-object ID detection setting, which is the same setting as zero-shot OOD detection. For the datasets, we use ImageNet-1K validation data [2] as ID, and iNaturalist [33], SUN [36], PLACES [39], and TEXTURE [1] as OOD, following the existing work [15]. For comparison methods, we also follow the comparison methods of MCM [23].

We show the results in Table 2. For the comparison with supervised learning models, our proposed GL-MCM is comparable or superior to them. Considering that supervised learning requires fine-tuning and GL-MCM is training-free, these results are very satisfactory. As for the comparison with MCM, GL-MCM outperforms it (except for the Texture dataset). We attribute this improvement to two factors. The first is that for single-object images, the performance of ID detection improves by focusing on the characteristic local area in addition to the global area. The second is that even in datasets assumed as "single-object datasets", some images contain OOD objects, such as people. From this result, we find that our proposed GL-MCM can also achieve sufficient performance in common single-object settings.

4.4. Analysis

Ablation of other score functions. To validate the effectiveness of GL-MCM, we experiment with different

score functions. We compute score functions in seven ways:

- (i) Entropy: the negative entropy of softmax scaled cosine similarities for both global and local scores. Formally, $S_{\text{entropy}} = -(H(\mathbf{p}) + \max_i(H(\mathbf{p}_i)))$, where \mathbf{p} and \mathbf{p}_i denote the K dimension output probability of the global feature \mathbf{x}' and the local feature \mathbf{x}'_i respectively. $H(\cdot)$ denotes the entropy function.
- (ii) Var: the variance of the cosine similarities for both global and local scores. Formally, $S_{\text{var}} = V(\mathbf{s}) + \max_i(V(\mathbf{s}_i))$, where \mathbf{s} and \mathbf{s}_i denote the K dimension cosine similarity of the global feature and the local feature. $V(\cdot)$ denotes the variance function.
- (iii) Cos: the maximum cosine similarities for both global and local scores. Formally, $S_{\text{cos}} = \max_t(\text{sim}(\mathbf{x}', \mathbf{y}_t)) + \max_{t,i}(\text{sim}(\mathbf{x}'_i, \mathbf{y}_t))$.
- (iv) Global or Local MCM: the higher score of either the global or local confidence score. Formally, $S_{\text{G-or-L-MCM}} = \max(S_{\text{MCM}}, S_{\text{L-MCM}})$
- (v) L-Class-Avg CM: the maximum class-wise average concept matching score for local information. Formally, we define the prediction label pred_i for each region i of the feature map as follows: $\text{pred}_i = \arg \max_t \frac{e^{\text{sim}(\mathbf{x}'_i, \mathbf{y}_t)/\tau}}{\sum_{c \in \mathcal{T}_{in}} e^{\text{sim}(\mathbf{x}'_i, \mathbf{y}_c)/\tau}}$. We define the set of the region i where $\text{pred}_i = t \in \mathcal{T}_{in}$ as $I(t)$. With $I(t)$, the score function $S_{\text{L-Class-avg}}$ is defined as follow:
$$S_{\text{L-Class-avg}} = \max_t \frac{1}{|I(t)|} \cdot \sum_{i \in I(t)} \frac{e^{\text{sim}(\mathbf{x}'_i, \mathbf{y}_t)/\tau}}{\sum_{c \in \mathcal{T}_{in}} e^{\text{sim}(\mathbf{x}'_i, \mathbf{y}_c)/\tau}}. \quad (7)$$
- (vi) L-Class-Avg CM + MCM: the ensemble method with L-Class-AVG CM and MCM. Formally, the score function is $S_{\text{L-Class-avg}} + S_{\text{MCM}}$.

Table 3: Comparison with other score functions. The score denotes the average score of the performances on five OOD datasets in Table 1. We use CLIP-B/16 as the backbone.

Method	ID: COCO		ID: VOC	
	FPR95↓	AUROC↑	FPR95↓	AUROC↑
(i) Entropy	80.03	76.23	55.16	90.17
(ii) Var	80.56	75.38	44.46	91.35
(iii) Cos	90.86	80.11	55.16	90.17
(iv) Global or Local MCM	63.38	84.96	47.30	89.15
(v) L-Class-Avg CM	64.27	81.58	59.70	86.04
(vi) L-Class-Avg CM + MCM	63.39	88.28	37.94	93.36
(vii) L-MCM + MCM (GL-MCM)	61.72	88.10	31.12	93.81

- (vii) L-Max CM + MCM: GL-MCM (ours). Formally, $S_{GL-MCM} = S_{L-MCM} + S_{MCM}$.

In Table 3, we show the results with these score functions. We find that (vii) GL-MCM gives the best results compared to other score functions. Especially even though the score functions of (vii) and (vi) are similar, (vii) GL-MCM is slightly superior to (vi) L-Class-Avg CM + MCM. This is because the class average score takes into account some low matching scores and might not produce high ID confidence.

Visualization of the alignment maps. In Fig. 6, we visualize the alignment maps for MCM and L-MCM. Specifically, for MCM, we show the alignment map of the CLIP-B/16 encoder, and for L-MCM, we show the region with the local maximum concept matching score. Note that it is not possible to visualize the attention map of GL-MCM, but it is regarded as a combination of both these maps. In the case of an ID object captured locally, MCM does not pool its features well, as shown at the top of Fig. 6. On the other hand, L-MCM cannot adequately take into account the features of objects captured globally, as shown at the bottom of Fig. 6. Therefore, GL-MCM, which incorporates these two approaches, can reinforce these two weaknesses.

5. Discussion

5.1. Limitations

ID classification. ID detection is a task of distinguishing ID and OOD, which is the same as OOD detection and does not focus on improving close-set ID recognition accuracies. The usage of this task is to exclude OOD images from the scraped images before the annotators assign class labels, so this task can reduce considerable human effort and help annotators even without the ability to close-set classifications. However, considering the application of GL-MCM to ID classification, GL-MCM can output both global and local classes, while the conventional CLIP outputs only global classes. Therefore, GL-MCM would also be very useful for assisting with ID labeling.

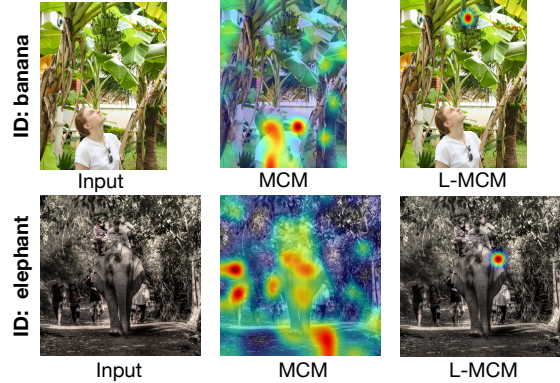


Figure 6: Visualization of the alignment maps of MCM and L-MCM.

Need of the model with the rich local visual-text alignment. This method relies on models with strong local visual-text alignment capabilities, such as CLIP’s Image Encoder. Therefore, it is difficult to apply this method to models that do not have such local visual-text alignment. However, since many methods are currently being proposed based on CLIP, our work provides a beneficial insight into the research of vision-language research fields.

5.2. Usage of zero-shot ID detection

Since zero-shot ID detection is the task we first propose in this work, we show the effective usages in the following. The best way to use ID detection is to exclude OOD images when cleaning collected data, as described in the Introduction. Especially when collecting rare classes that must not be missed, such images should be considered ID images even if OOD objects are included in the image. If you want to collect images of rare classes showing only ID objects, you can manually crop the extracted ID images so that only ID objects appear. Also, even if you want to collect more fine-grained classes (*e.g.*, animal or plant species) CLIP might not identify, you can use our ID detector with supercategory classes (*e.g.*, bird, dog, cat) for collecting ID data, then you can annotate them manually.

6. Conclusion

In this paper, we propose a novel problem setting called ID detection, where we identify images containing ID objects as ID images, even if they contain OOD objects, and images lacking ID objects as OOD images. To solve this problem, we present Global-Local Maximum Concept Matching (GL-MCM), based on both global and local visual-text alignments. Extensive experiments demonstrate that GL-MCM outperforms comparison methods on real-world multi-object and single-object datasets.

References

- [1] Mircea Cimpoi, Subhransu Maji, Iasonas Kokkinos, Sammy Mohamed, and Andrea Vedaldi. Describing textures in the wild. In *CVPR*, 2014. 5, 7
- [2] Jia Deng, Wei Dong, Richard Socher, Li-Jia Li, Kai Li, and Li Fei-Fei. Imagenet: A large-scale hierarchical image database. In *CVPR*, 2009. 1, 7
- [3] Alexey Dosovitskiy, Lucas Beyer, Alexander Kolesnikov, Dirk Weissenborn, Xiaohua Zhai, Thomas Unterthiner, Mostafa Dehghani, Matthias Minderer, Georg Heigold, Sylvain Gelly, Jakob Uszkoreit, and Neil Houlsby. An image is worth 16x16 words: Transformers for image recognition at scale. In *ICLR*, 2021. 6
- [4] Xuefeng Du, Gabriel Gozum, Yifei Ming, and Yixuan Li. Siren: Shaping representations for detecting out-of-distribution objects. In *NeurIPS*, 2022. 3
- [5] Xuefeng Du, Xin Wang, Gabriel Gozum, and Yixuan Li. Unknown-aware object detection: Learning what you don't know from videos in the wild. In *CVPR*, 2022. 3
- [6] Sepideh Esmailpour, Bing Liu, Eric Robertson, and Lei Shu. Zero-shot out-of-distribution detection based on the pretrained model clip. In *AAAI*, 2022. 1, 2, 3, 6
- [7] Mark Everingham, Luc Van Gool, Christopher KI Williams, John Winn, and Andrew Zisserman. The pascal visual object classes (voc) challenge. *IJCV*, 88:303–308, 2009. 2, 5
- [8] Stanislav Fort, Jie Ren, and Balaji Lakshminarayanan. Exploring the limits of out-of-distribution detection. In *NeurIPS*, 2021. 1, 2, 3, 6, 7
- [9] ZongYuan Ge, Sergey Demyanov, Zetao Chen, and Rahil Garnavi. Generative openmax for multi-class open set classification. *arXiv preprint arXiv:1707.07418*, 2017. 2
- [10] Kaiming He, Xiangyu Zhang, Shaoqing Ren, and Jian Sun. Deep residual learning for image recognition. In *CVPR*, 2016. 6
- [11] Dan Hendrycks, Steven Basart, Mantas Mazeika, Mohammadreza Mostajabi, Jacob Steinhardt, and Dawn Song. Scaling out-of-distribution detection for real-world settings. In *ICML*, 2022. 2, 3, 6
- [12] Dan Hendrycks and Kevin Gimpel. A baseline for detecting misclassified and out-of-distribution examples in neural networks. In *ICLR*, 2017. 2, 7
- [13] Dan Hendrycks, Xiaoyuan Liu, Eric Wallace, Adam Dziedziec, Rishabh Krishnan, and Dawn Song. Pretrained transformers improve out-of-distribution robustness. In *ACL*, 2020. 2
- [14] Rui Huang, Andrew Geng, and Yixuan Li. On the importance of gradients for detecting distributional shifts in the wild. In *NeurIPS*, 2021. 2
- [15] Rui Huang and Yixuan Li. Mos: Towards scaling out-of-distribution detection for large semantic space. In *CVPR*, 2021. 2, 5, 7
- [16] Polina Kirichenko, Pavel Izmailov, and Andrew G Wilson. Why normalizing flows fail to detect out-of-distribution data. In *NeurIPS*, 2020. 2
- [17] Kimin Lee, Kibok Lee, Honglak Lee, and Jinwoo Shin. A simple unified framework for detecting out-of-distribution samples and adversarial attacks. In *NeurIPS*, 2018. 2
- [18] Junnan Li, Ramprasaath Selvaraju, Akhilesh Gotmare, Shafiq Joty, Caiming Xiong, and Steven Chu Hong Hoi. Align before fuse: Vision and language representation learning with momentum distillation. In *NeurIPS*, 2021. 3
- [19] Shiyu Liang, Yixuan Li, and Rayadurgam Srikant. Enhancing the reliability of out-of-distribution image detection in neural networks. In *ICLR*, 2018. 2
- [20] Tsung-Yi Lin, Michael Maire, Serge Belongie, James Hays, Pietro Perona, Deva Ramanan, Piotr Dollár, and C Lawrence Zitnick. Microsoft coco: Common objects in context. In *ECCV*, 2014. 2, 5
- [21] Weitang Liu, Xiaoyun Wang, John Owens, and Yixuan Li. Energy-based out-of-distribution detection. In *NeurIPS*, 2020. 2, 7
- [22] Shu Manli, Nie Weili, Huang De-An, Yu Zhiding, Goldstein Tom, Anandkumar Anima, and Xiao Chaowei. Test-time prompt tuning for zero-shot generalization in vision-language models. In *NeurIPS*, 2022. 3
- [23] Yifei Ming, Ziyang Cai, Jiuxiang Gu, Yiyao Sun, Wei Li, and Yixuan Li. Delving into out-of-distribution detection with vision-language representations. In *NeurIPS*, 2022. 1, 2, 3, 4, 5, 6, 7
- [24] Eric Nalisnick, Akihiro Matsukawa, Yee Whye Teh, Dilan Gorur, and Balaji Lakshminarayanan. Do deep generative models know what they don't know? In *ICLR*, 2019. 2
- [25] Lawrence Neal, Matthew Olson, Xiaoli Fern, Weng-Keen Wong, and Fuxin Li. Open set learning with counterfactual images. In *ECCV*, 2018. 2
- [26] Poojan Oza and Vishal M Patel. C2ae: Class conditioned auto-encoder for open-set recognition. In *CVPR*, 2019. 2
- [27] Alexander Podolskiy, Dmitry Lipin, Andrey Bout, Ekaterina Artemova, and Irina Piontkovskaya. Revisiting mahalanobis distance for transformer-based out-of-domain detection. In *AAAI*, 2021. 2
- [28] Alec Radford, Jong Wook Kim, Chris Hallacy, Aditya Ramesh, Gabriel Goh, Sandhini Agarwal, Girish Sastry, Amanda Askell, Pamela Mishkin, Jack Clark, et al. Learning transferable visual models from natural language supervision. In *ICML*, 2021. 1, 3
- [29] Tal Ridnik, Emanuel Ben-Baruch, Asaf Noy, and Lihi Zelnik-Manor. Imagenet-21k pretraining for the masses. In *NeurIPS Datasets and Benchmarks Track*, 2021. 5
- [30] Kuniaki Saito, Kihyuk Sohn, Xiang Zhang, Chun-Liang Li, Chen-Yu Lee, Kate Saenko, and Tomas Pfister. Pic2word: Mapping pictures to words for zero-shot composed image retrieval. *arXiv preprint arXiv:2302.03084*, 2023. 3
- [31] Ximeng Sun, Ping Hu, and Kate Saenko. Dualcoop: Fast adaptation to multi-label recognition with limited annotations. In *NeurIPS*, 2022. 3
- [32] Yiyao Sun, Yifei Ming, Xiaojin Zhu, and Yixuan Li. Out-of-distribution detection with deep nearest neighbors. In *ICML*, 2022. 2
- [33] Grant Van Horn, Oisín Mac Aodha, Yang Song, Yin Cui, Chen Sun, Alex Shepard, Hartwig Adam, Pietro Perona, and Serge Belongie. The inaturalist species classification and detection dataset. In *CVPR*, 2018. 5, 7

- [34] Haoqi Wang, Zhizhong Li, Litong Feng, and Wayne Zhang. Vim: Out-of-distribution with virtual-logit matching. In *CVPR*, 2022. [2](#)
- [35] Haoran Wang, Weitang Liu, Alex Bocchieri, and Yixuan Li. Can multi-label classification networks know what they don't know? In *NeurIPS*, 2021. [3](#), [5](#)
- [36] Jianxiong Xiao, James Hays, Krista A Ehinger, Aude Oliva, and Antonio Torralba. Sun database: Large-scale scene recognition from abbey to zoo. In *CVPR*, 2010. [5](#), [7](#)
- [37] Keyang Xu, Tongzheng Ren, Shikun Zhang, Yihao Feng, and Caiming Xiong. Unsupervised out-of-domain detection via pre-trained transformers. In *ACL*, 2021. [2](#)
- [38] Jingkang Yang, Pengyun Wang, Dejian Zou, Zitang Zhou, Kunyuan Ding, Wenxuan Peng, Haoqi Wang, Guangyao Chen, Bo Li, Yiyao Sun, Xuefeng Du, Kaiyang Zhou, Wayne Zhang, Dan Hendrycks, Yixuan Li, and Ziwei Liu. Openood: Benchmarking generalized out-of-distribution detection. In *NeurIPS Datasets and Benchmarks Track*, 2022. [2](#)
- [39] Bolei Zhou, Agata Lapedriza, Aditya Khosla, Aude Oliva, and Antonio Torralba. Places: A 10 million image database for scene recognition. *TPAMI*, 40(6):1452–1464, 2017. [7](#)
- [40] Chong Zhou, Chen Change Loy, and Bo Dai. Extract free dense labels from clip. In *ECCV*, 2022. [2](#), [3](#), [4](#)
- [41] Kaiyang Zhou, Jingkang Yang, Chen Change Loy, and Ziwei Liu. Conditional prompt learning for vision-language models. In *CVPR*, 2022. [3](#)
- [42] Kaiyang Zhou, Jingkang Yang, Chen Change Loy, and Ziwei Liu. Learning to prompt for vision-language models. *IJCV*, 2022. [3](#)